



Residual stresses and high cycle fatigue properties of friction stir welded SiCp/AA2009 composites



D.R. Ni^a, D.L. Chen^{b,*}, B.L. Xiao^a, D. Wang^a, Z.Y. Ma^{a,*}

^aShenyang National Laboratory for Materials Science, Institute of Metal Research, Chinese Academy of Sciences, 72 Wenhua Road, Shenyang 110016, China

^bDepartment of Mechanical and Industrial Engineering, Ryerson University, 350 Victoria Street, Toronto, Ontario M5B 2K3, Canada

ARTICLE INFO

Article history:

Received 24 September 2012

Received in revised form 10 May 2013

Accepted 22 May 2013

Available online 31 May 2013

Keywords:

Metal matrix composites (MMCs)

Friction stir welding

Residual stress

Fatigue

Fracture

ABSTRACT

3 mm thick rolled SiCp/AA2009 sheet in T351 condition was subjected to friction stir welding (FSW). FSW generated high residual stresses with the peak value occurring in the weld center. While the FSW joint showed a shorter fatigue life than the base material (BM) at stress amplitudes higher than 150 MPa, it had a fatigue life equivalent to the BM at lower stress amplitudes with a fatigue limit of about 100 MPa. In the BM the fatigue crack initiated at the SiCp agglomeration or inclusions; however, in the joint the initiation zone was mainly characterized by the formation of dimples.

© 2013 Elsevier Ltd. All rights reserved.

1. Introduction

Aluminum matrix composites (AMCs) are attractive materials particularly in the aerospace and automotive industries due to their advantages over unreinforced aluminum alloys [1–3]. Compared to the long fiber reinforced AMCs, particle and whisker reinforced AMCs are rapidly developed because of their low costs, isotropic properties, and desirable deformability. The structural application of AMCs involves inevitably welding and joining during manufacturing. However, with the addition of ceramic particles, it is hard to achieve defect-free welds using conventional fusion welding techniques [4,5]. This hinders their development and application to some extent.

Friction stir welding (FSW), as an effective solid-state joining technique, has been successfully used for welding aluminum and magnesium alloys [6,7]. This solid state welding technique may avoid the drawbacks of the fusion welding and therefore, could produce sound AMC joints. For example, Storjohann et al. [4] reported that the fusion welding could not produce defect-free welds of Al₂O₃/AA6061 and SiC/AA2024 composites due to the decomposition of ceramic particles or the rapid reaction of the particles with molten Al matrix, but FSW led to good joints without much degradation of the microstructure. Recently, more and more investiga-

tions on FSW of particles reinforced AMCs were reported, including Al₂O₃/AA7005 [8,9], Al₂O₃/AA6061 [9–13], SiC/AA2009 [14–16], B₄C/AA6063 [17], TiB₂/Al [18], Mg₂Si/Al–9.7Mg–5.5Si [19], TiC/Al [20], and SiC/AA356 [21], with the microstructures and mechanical properties of the FSW AMCs carefully analyzed.

For the industrial applications of FSW joints, it is crucial to understand the following two issues thoroughly. First, the fatigue properties are required to determine the durability of the joints, and this is fundamental in influencing the structural integrity and performance of FSW joints. Second, the frictional heating and severe plastic deformation involved in FSW generate significant residual stresses, and this has been extensively demonstrated in the FSW of aluminum alloys [22–31], magnesium alloys [32], steels [33,34], and titanium alloys [35]. Although the residual stress in the FSW joints may be greatly lower than that in the fusion ones, they were reported to produce large effects on the fatigue crack growth in the joint [36–43].

At present the studies on the fatigue properties of the FSW AMCs are limited, with the focus primarily on the FSW joints of as-cast Al₂O₃p/AMCs [8,12,13,44–46], including the fatigue crack propagation resistance [44,45], low cycle fatigue behavior [8,12], and high cycle fatigue behavior [13,46]. In particular, the investigations on the residual stress of the FSW AMCs are extremely limited [44]. It is unclear how the residual stress in the FSW AMC joints affects their fatigue resistance.

In the present study, 3 mm thick 17 vol.% SiCp/AA2009 sheets were subjected to FSW and detailed residual stress and high cycle

* Corresponding authors. Tel.: +1 4169795000x6487; fax: +1 4169795265 (D.L. Chen), tel./fax: +86 24 83978908 (Z.Y. Ma).

E-mail addresses: dchen@ryerson.ca (D.L. Chen), zym@imr.ac.cn (Z.Y. Ma).

fatigue behavior investigations. The aim is to understand the effect of residual stresses on the high cycle fatigue fracture behavior of the FSW AMC joints.

2. Materials and methods

AA2009 composite reinforced with 17 vol.% SiCp was produced by powder metallurgy technique. The SiCp with an average particle size of 7 μm were adopted. The chemical composition of the AA2009 alloy was 4.26Cu–1.61Mg–0.01Si–0.009Fe (wt.%). The hot pressed ingot was first extruded and subsequently rolled into 3 mm thick sheets with the rolling direction perpendicular to the extrusion direction. The rolled sheet was T351-treated (solutionized at 502 $^{\circ}\text{C}$ for 1 h, water quenched, cold rolled with 15% reduction and then aged at room temperature for more than 1 month) and cut into pieces of 95 \times 400 mm for FSW, with the length direction perpendicular to the rolling direction. The composite pieces were welded at a tool rotational rate of 1000 rpm and a welding speed of 50 mm/min. A cermet tool with a shoulder 14 mm in diameter and a cylindrical pin 5 mm in diameter and 2.7 mm in length was adopted.

Specimens for microstructural examinations were cross sectioned perpendicular to the FSW direction. The microstructures were examined using optical microscopy (OM), scanning electron microscopy (SEM, Quanta 600), and transmission electron microscopy (TEM, FEI TECNAIG20). The specimens for OM and SEM were prepared by mechanical grinding and polishing. The OM specimens were not etched but the SEM specimens were etched with Keller's reagent for the purpose of observing the SiCp distribution and morphology. Thin foils for TEM were cut from the base material (BM), nugget zone (NZ), and heat-affected zone (HAZ), respectively, and thinned by ion milling.

A specimen for the residual stress examination with a length of 40 mm (Y axis) and a width of 120 mm (X axis) was cut from a welded sheet (Fig. 1). X-ray diffraction (XRD) method was used to measure the residual stress in the upper surface of the FSW joint. Prior to measurement, the specimen was prepared by simply removing the toe flash. The measurements were conducted across the joint (X axis) with an interval of 1.5 mm using a PANalytical X-ray diffractometer. In order to estimate the magnitude of the surface residual stress, the lattice strains were assessed on Al (331). The details regarding the measurement conditions are shown in Table 1.

The hardness profiles were produced along the mid-thickness of the sheet at an interval of 0.5 mm on the cross section of the weld by using a computerized Buehler hardness tester under a load of 1000 g for 15 s. Tensile specimens with a parallel section of 32 \times 5.6 \times 3 mm were machined perpendicular to the FSW direc-

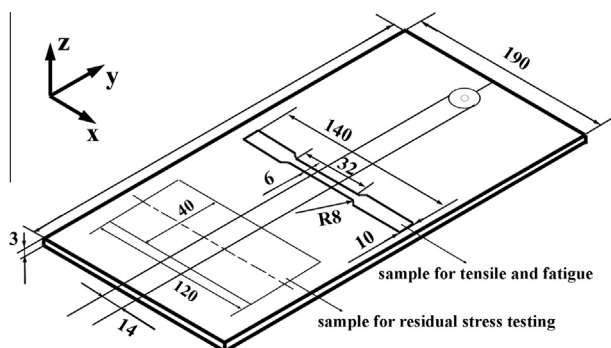


Fig. 1. Sampling schematic of FSW SiCp/AA2009 joint for residual stress, fatigue, and tensile testing.

Table 1
Residual stress measuring conditions for X-ray diffraction technique.

| X-ray diffractometer | PANalytical X'pert pro-MRD |
|--------------------------------|----------------------------------|
| Point interval | 1.5 mm |
| Point Size | \varnothing 0.3 mm |
| Model | PW3040/60 |
| <i>1. Measuring conditions</i> | |
| X-ray tube target | Cu |
| X-ray tube voltage | 45 kV |
| X-ray tube amperage | 40 mA |
| <i>2. Diffracting grating</i> | |
| Diffracting plane | (331) |
| Diffracting angle | 112.248 $^{\circ}$ (2θ) |
| Diffracting angle range | 5.9 $^{\circ}$ |
| Incident | Mono-capillary 0.3 mm |
| Diffracted beam optics | Parallel plate collimator 0.027 |
| Rad with soller slit | 0.04 rad and Nickel filter |

tion, as shown in Fig. 1. The specimens were electrical discharge machined and ground with SiC papers up to grit #600 to get rid of the machining marks and to achieve a smooth surface. Tensile tests were conducted at room temperature at a strain rate of $1 \times 10^{-3} \text{ s}^{-1}$.

High cycle fatigue (HCF) tests were conducted using a computerized Instron fatigue testing system (Instron 8801) with the same specimen dimension and preparation method as those for the tensile specimens. Sine waveform with a strain ratio of $R = 0$ was applied at a frequency of 50 Hz. At least two specimens were tested at each stress level. After the fatigue tests, the crack initiation sites and propagation mechanisms were examined using SEM (JEOL JSM-6380LV) coupled with energy-dispersive X-ray spectroscopy (EDS).

3. Results

3.1. Microstructure

Fig. 2 shows a typical cross-sectional macrograph of the FSW joint. As can be seen, a sound FSW SiCp/AA2009 joint was achieved. The NZ in the weld was obvious but the thermomechanically-affected zone (TMAZ) and the HAZ were indistinct. The optical microstructure observation showed that SiCp were more homogeneously distributed in the NZ than in the BM (Fig. 3a and b). The SEM examinations revealed that polygonal SiCp with the long axis parallel to the rolling direction were distributed in the BM (Fig. 3c); however, in the NZ the size and the aspect ratio of SiCp were decreased and the edges and corners of the SiCp were blunted (Fig. 3d).

Fig. 4 shows the TEM microstructure of various regions in the FSW joint. The BM was featured by a high density of dislocations, without visible precipitates being detected (Fig. 4a). However, a small amount of coarse precipitates and lower density of dislocations were observed in the NZ (Fig. 4b). Unlike the BM and the NZ, the HAZ was characterized by many coarse precipitates and few dislocations (Fig. 4c). These precipitates could be divided into two kinds according to their morphologies and sizes: fine needle-shaped precipitates and coarse granular precipitates. According to previous investigations [15,47,48], the fine needle-shaped pre-



Fig. 2. Cross-sectional macrostructures of FSW SiCp/AA2009 joint.

Download English Version:

<https://daneshyari.com/en/article/776873>

Download Persian Version:

<https://daneshyari.com/article/776873>

[Daneshyari.com](https://daneshyari.com)